PHYSICAL REVIEW D VOLUME 53, NUMBER 5 1 MARCH 1996

Electroweak radiative corrections to $t\bar{t} \to H_0H_0$ in the two-Higgs-doublet model

Sun La-Zhen and Liu Yao-Yang
Department of Modern Physics, University of Science and Technology of China, Hefei, Anhui, 230026, People's Republic of China
(Received 14 August 1995)

Electroweak radiative one-loop corrections to Higgs boson pair production in $t\bar{t}$ fusion processes are calculated in the two-Higgs-doublet extension of the standard model. The numerical size of the nonstandard corrections is discussed for the process $t\bar{t} \to H_0H_0$. The relative difference between the predictions of the two-Higgs-doublet model and the minimal standard model for a light scalar M_{H_1} and heavy M_{H_2} and M_Φ easily exceeds -10% in the forward and backward directions. In particular the angular-dependence corrections owing to the nonstandard Higgs bosons get larger where the box and cubic Higgs boson vertex corrections constitute the dominant part of the radiative corrections.

PACS number(s): 12.60.Cn, 12.15.Lk, 14.80.Cp

I. INTRODUCTION

Precision measurements of electroweak observables in combination with corresponding radiative corrections allow upper limits to be set on the mass of the top quark, which should be lighter than about 200 GeV in the minimal standard model (MSM) [1]. Recent experimental evidence shows the top quark mass to be in the range 174 ± 17 GeV [2]. However, the predictions of the standard model depend very weakly on the mass of the Higgs boson. The present experimental information on the Higgs sector is rather poor. The only essential restriction is that the ρ parameter $\rho = M_W^2/(M_Z^2 \cos^2\theta_W)$ be close to 1. In part for this reason, the simplest extension of the MSM is the two-Higgs-doublet model (THDM), which keeps not only the important relation $\rho = 1$, but also eliminates flavor-changing neutral currents (FCNC's) [3]. As required for the THDM, the THDM has an extended Higgs sector with two Higgs doublets of opposite hypercharges Φ_1, responsible for the mass of the charged leptons and the down-type quarks, and Φ_2, which gives a mass to the up-type quarks. After the Higgs mechanism, there remain six parameters in the THDM; they are two CP-even Higgs boson masses M_{H_0} and M_{H_1}, one CP-odd Higgs boson mass M_{H_2}, one pair charged Higgs boson mass $M_{\Phi^\pm}$, and the mixing angles α and β. α is the mixing angle of the CP-even Higgs bosons H_0 and H_1; $\tan\beta = V_2/V_1$ is the ratio of the vacuum expectation values (VEV's) of the two Higgs fields. One of the neutral scalars (H_0) behaves similarly to that of the standard model.

A lower limit on the Higgs boson mass of 58.4 GeV at 95% C.L. for the MSM has recently been set at the CERN e^+e^- collider LEP [4]. In the search for this particle, LEP will cover the mass range up to approximately 90 GeV. New accelerators such as the $p\bar{p}$ colliders [the CERN Large Hadron Collider (LHC), for example] will be needed to continue the search if the Higgs boson is heavier than the Z mass. The production of Higgs boson pairs is preferable at future $p\bar{p}$ or pp collisions. For heavier top quarks and Higgs boson, the $t\bar{t}$ fusion process $t\bar{t} \to H_0H_0$ overtakes $WW/ZZ \to H_0H_0$ [5], since the $t\bar{t}H_0$ coupling is m_t/M_W and the $t\bar{t}$ fusion process, the amplitude M_s for s-channel Higgs boson exchange, is proportional to the square of its mass in the SM. At the tree level the THDM is identical to the SM. The THDM differs from the SM, however, in that radiative corrections often depend rather sensitively on the details of the Higgs sector. Since the general THDM has no theoretical constraints on all its six parameters, it is particularly flexible in radiative corrections to the process $t\bar{t} \to H_0H_0$. Therefore the radiative corrections can be enhanced or reduced and may show large deviations from that in the MSM by adjusting β and other parameters.

In this paper we extend the on-shell renormalization scheme of the SM [6] to the THDM. In particular, we discuss the radiative corrections to the process $t\bar{t} \to H_0H_0$ arising from the additional Higgs bosons. We specify the THDM with $\tan\beta = V_2/V_1 >> 1$, $\alpha = \beta$, and flavor-changing neutral currents at the tree level are avoided by having one doublet (V_2) couple only to the up-type quark and leptons and the other (V_1) only to the down-type quark. The neutral Higgs boson H_0 has the same coupling as the MSM Higgs boson. Note that the masses of the Higgs ghosts χ and $\psi_\pm$ are M_Z and M_W also the same with that in the MSM in the 't Hooft–Feynman gauge. The electroweak radiative corrections in the context of the MSM have been given in Ref. [7] so that we can evaluate a meaningful additional electroweak correction within the THDM and keep the results of the MSM corrections as one part of the THDM corrections.

II. NOTATION AND LOWEST ORDER

We consider the reaction

$$t(p_1,\sigma_1) + \bar{t}(p_2,\sigma_2) \to H_0(p_3) + H_0(p_4) \ ,$$

where $\sigma_{1,2} = +\frac{1}{2}, -\frac{1}{2}$ and p_i are the momenta of the incoming quark and outgoing Higgs bosons. The Mandelstam variables are defined by

$$s = (p_1 + p_2)^2 = (p_3 + p_4)^2 \ , \quad (1)$$

$$t = (p_1 - p_3)^2 = (p_2 - p_4)^2 \ , \quad (2)$$

$$u = (p_1 - p_4)^2 = (p_2 - p_3)^2 \ . \quad (3)$$

The momenta read, in the center-of-mass system,

$$p_1 = \left(\frac{\sqrt{s}}{2}, \sqrt{\frac{s}{4} - m_t^2}, 0, 0\right) \ , \quad (4)$$

$$p_2 = \left(\frac{\sqrt{s}}{2}, -\sqrt{\frac{s}{4} - m_t^2}, 0, 0\right) \ , \quad (5)$$

$$p_3 = \left(\frac{\sqrt{s}}{2}, \sqrt{\frac{s}{4} - M_{H_0}^2}\cos\theta, \sqrt{\frac{s}{4} - M_{H_0}^2}\sin\theta, 0\right) \ , \quad (6)$$

$$p_4 = \left(\frac{\sqrt{s}}{2}, -\sqrt{\frac{s}{4} - M_{H_0}^2}\cos\theta, -\sqrt{\frac{s}{4} - M_{H_0}^2}\sin\theta, 0\right) \ . \quad (7)$$

Here θ is the scattering angle between the top quark and the Higgs boson.

We decompose the amplitude M into invariant functions F_i and standard matrix elements M_i. Using Dirac algebra and the Dirac equation for the amplitude, M can be reduced to

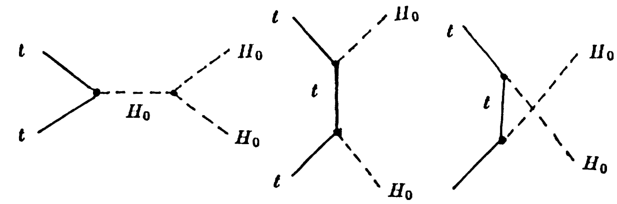

FIG. 1. Born diagrams for $t\bar{t} \to H_0 H_0$.

$$M^{\rm THDM}(\sigma_1, \sigma_2, s, t, u) = \sum_{i=0}^{7} F_i^{\rm THDM}(s,t,u) M_i(\sigma_1, \sigma_2, s, t, u) \ , \quad (8)$$

with

$$M_0 = \bar{V}(p_2)U(p_1) \ , \quad M_1 = \bar{V}(p_2)\gamma_5 U(p_1) \ ,$$

$$M_2 = \bar{V}(p_2)\not{p}_3 U(p_1) \ , \quad M_3 = \bar{V}(p_2)\gamma_5\not{p}_3 U(p_1) \ ,$$

$$M_4 = \bar{V}(p_2)\not{p}_4 U(p_1) \ , \quad M_5 = \bar{V}(p_2)\gamma_5\not{p}_4 U(p_1) \ ,$$

$$M_6 = \bar{V}(p_2)\not{p}_4\not{p}_3 U(p_1) \ , \quad M_7 = \bar{V}(p_2)\not{p}_3\not{p}_4 U(p_1) \ .$$

Then we can write the differential cross section

$$\left(\frac{d\sigma}{d\cos\theta}\right)^{\rm THDM} = \sum_{\sigma_1\sigma_2} \frac{2\sqrt{\frac{s}{4} - m_t^2}\sqrt{\frac{s}{4} - M_{H_0}^2}}{64\pi s\left(\frac{s}{4} - m_t^2\right)} |M^{\rm THDM}(\sigma_1, \sigma_2, s, t, u)|^2 \ .$$

The three tree diagrams (Fig. 1) yield the Born amplitude $M_{\rm Born}$:

$$M_{\rm Born} = i g_{ttH_0} g_{H_0H_0H_0} \frac{M_0}{s - M_{H_0}^2} + i g_{ttH_0}^2 \left[\frac{2m_t(M_0 - M_2)}{t - m_t^2} + \frac{2m_t(M_0 - M_4)}{u - m_t^2}\right] \ ,$$

with

$$g_{ttH_0} = \frac{-igm_t}{2M_W} \ , \quad g_{H_0H_0H_0} = \frac{-i3gM_{H_0}^2}{2M_W} \ .$$

The behavior of the lowest-order cross sections on c.m. energy is illustrated in Fig. 2, $\sigma_{\rm Born}(M_{H_0})$, as a function of M_{H_0} for $m_t = 195$, 175, and 155 GeV and $\sqrt{s} = 1$ TeV. We can find that the cross sections drop with increasing M_{H_0} and are large for smaller M_{H_0} or large m_t. The spikes arise from thresholds at $M_{H_0} \sim 470$ GeV. This is due mainly to $\sigma_s \propto M_{H_0}^4 \sqrt{s/4 - M_{H_0}^2}/(s - M_{H_0}^2)$ in the cross sections originating from the s channel.

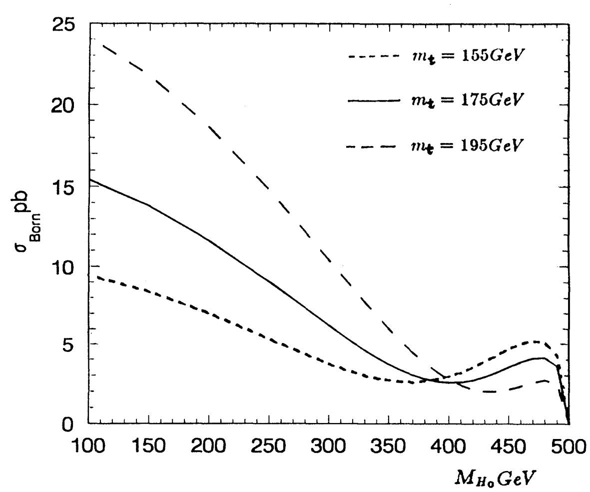

FIG. 2. Lowest order cross section for various masses of the top quark.

III. RADIATIVE CORRECTIONS

We have performed the calculation of radiative corrections in the 't Hooft–Feynman gauge applying the complete on-shell renormalization scheme as worked out for the MSM in Ref. [6]. There fields are normalized in such a way that residues of all renormalized propagators are equal to 1. Consequently no external wave function renormalization is required. At $O(\alpha)$ we therefore have to take into account corrections to the H_0 and t propagators, corrections to the H_0 and t vertices of the incoming top quarks and the outgoing Higgs boson and box contributions with the exchange of the additional Higgs bosons.

Since the QED corrections in both the THDM and MSM are identical and can be found in Ref. [7], we discuss only the weak corrections here. In our specific THDM case, we can split the one-loop weak corrections up into parts. One part is from the MSM, which has already been presented in [7], and the other part is from the nonstandard (NS) Higgs bosons part of the THDM. For a consistent treatment of the virtual one-loop corrections, the squared transition matrix element $|M|^2$ has to be expanded to a power series of the coupling constant to

$$|M|^{2\,\mathrm{THDM}} = |M_{\mathrm{Born}}|^2 + 2\mathrm{Re}|\delta M^{\mathrm{THDM}} M^{\dagger}_{\mathrm{Born}}| + \text{higher order} . \tag{9}$$

We denote the $O(\alpha)$ correction δM^{THDM} to the matrix element by

$$\begin{aligned}\delta M(s,t,u)^{\mathrm{THDM}} &= \sum_{i=0}^{7} \delta F_i^{\mathrm{THDM}} M_i(s,t,u)\\ &= \delta M^{\mathrm{SM}} + \delta M^{\mathrm{NS}}\\ &= \sum_{i=0}^{7} \delta F_i^{\mathrm{SM}} M_i(s,t,u)\\ &\quad + \sum_{i=0}^{7} \delta F_i^{\mathrm{NS}} M_i(s,t,u) .\end{aligned}$$

The invariant functions δF_i are calculated in terms of standard tensor integrals. The scalar one-loop integrals are evaluated using the methods of [8]. Where UV divergences are regularized by calculating in dimensions of $4-2\epsilon$, we treat IR divergences by the introduction of an infinite small photon mass λ. Of course, the λ dependence drops out when soft photon bremsstrahlung is added. The UV and IR finite differential cross sections including $O(\alpha)$ corrections in the soft photon approximation reads

$$\begin{aligned}\left(\frac{d\sigma}{d\cos\theta}\right)^{\mathrm{THDM}} &= \sum_{\sigma_1\sigma_2} \frac{2\sqrt{\frac{s}{4}-m_t^2}\sqrt{\frac{s}{4}-M_{H_0}^2}}{64\pi s\left(\frac{s}{4}-m_t^2\right)} [|M_{\mathrm{Born}}|^2(1+\delta_{\mathrm{SB}}) + 2\mathrm{Re}\{\delta M M^{\dagger}_{\mathrm{Born}}\}]\\ &= \left(\frac{d\sigma}{d\cos\theta}\right)_{\mathrm{Born}} (1+\delta_{\mathrm{SM}}+\delta_{\mathrm{NS}}) = \left(\frac{d\sigma}{d\cos\theta}\right)_{\mathrm{Born}} (1+\delta_{\mathrm{THDM}}) ,\end{aligned}$$

where δ_{SM} and δ_{SB} denote the relative electroweak corrections and the soft photonic bremsstrahlung correction factor in the MSM; δ_{NS} is the relative electroweak corrections of nonstandard Higgs bosons in the THDM. We now list the different contributions to δM^{NS}.

A. Self-energies

As already mentioned, we do not have to deal with the self-energies of external fields. The internal H_0 and top quark self-energies $\Sigma^{\mathrm{NS}}_{H_0H_0}(s)$ and $\Sigma^{\mathrm{NS}}_{tt}(t,u)$ arising from the nonstandard Higgs boson graphs in Fig. 3 contribute to δM^{NS} with

$$\delta M^{\mathrm{NS}}_{H_0H_0}(s) = -ig_{ttH_0}g_{H_0H_0H_0}M_0\left[\frac{\hat{\Sigma}^{\mathrm{NS}}_{H_0H_0}(s)}{(s-M_{H_0}^2)^2}\right] ,$$

$$\delta M^{\mathrm{NS}}_{tt}(t) = -ig^2_{ttH_0}\left[\frac{\bar{V}(p_2)(\not{p}_1-\not{p}_3+m_t)\hat{\Sigma}^{\mathrm{NS}}_{tt}(t)(\not{p}_1-\not{p}_3+m_t)U(p_1)}{(t-m_t^2)^2}\right] ,$$

$$\delta M^{\mathrm{NS}}_{tt}(u) = -ig^2_{ttH_0}\left[\frac{\hat{V}(p_2)(\not{p}_1-\not{p}_4+m_t)\hat{\Sigma}^{\mathrm{NS}}_{tt}(u)(\not{p}_1-\not{p}_4+m_t)U(p_1)}{(u-m_t^2)^2}\right] ,$$

where $\hat{\Sigma}^{\mathrm{NS}}_{H_0H_0}(s)$ and $\hat{\Sigma}^{\mathrm{NS}}_{tt}(t,u)$ denote the renormalized nonstandard Higgs boson and top quark self-energies:

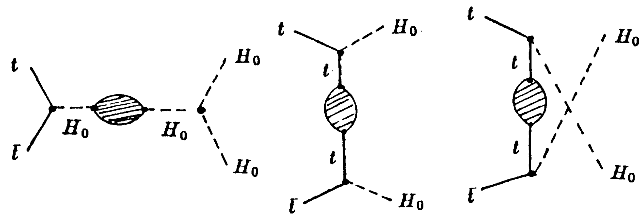

FIG. 3. Self-energy corrections.

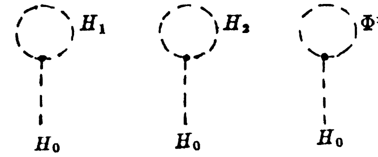

FIG. 4. Nonstandard Higgs tadpole graphs.

$$\hat{\Sigma}^{\rm NS}_{H_0H_0}(s) = \Sigma^{\rm NS}_{H_0H_0}(s) + (s - M^2_{H_0})\delta Z^{\rm NS}_{H_0} - \delta M^{2\ {\rm NS}}_{H_0}\ ,$$

$$\begin{aligned}\hat{\Sigma}^{\rm NS}_{tt}(t) = {}& (\not{p}_1 - \not{p}_3)\omega_- \Sigma^{L,{\rm NS}}_t(t) + (\not{p}_1 - \not{p}_3)\omega_+ \Sigma^{R,{\rm NS}}_t(t) + m_t \Sigma^{S,{\rm NS}}_t(t) \\ & + \delta Z^{L,{\rm NS}}_t(\not{p}_1 - \not{p}_3)\omega_- + \delta Z^{R,{\rm NS}}_t(\not{p}_1 - \not{p}_3)\omega_+ - \left[\frac{m_t}{2}(\delta Z^{L,{\rm NS}}_t + Z^{R^+,{\rm NS}}_t) + \delta m^{\rm NS}_t\right]\omega_- \\ & - \left[\frac{m_t}{2}(\delta Z^{R,{\rm NS}}_t + \delta Z^{L^+,{\rm NS}}_t) + \delta m^{\rm NS}_t\right]\omega_+\ ,\end{aligned}$$

$$\begin{aligned}\hat{\Sigma}^{\rm NS}_{tt}(u) = {}& (\not{p}_1 - \not{p}_4)\omega_- \Sigma^{L,{\rm NS}}_t(u) + (\not{p}_1 - \not{p}_4)\omega_+ \Sigma^{R,{\rm NS}}_t(u) + m_t \Sigma^{S,{\rm NS}}_t(u) \\ & + \delta Z^{L,{\rm NS}}_t(\not{p}_1 - \not{p}_4)\omega_- + \delta Z^{R,{\rm NS}}_t(\not{p}_1 - \not{p}_4)\omega_+ - \left[\frac{m_t}{2}(\delta Z^{L,{\rm NS}}_t + \delta Z^{R^+,{\rm NS}}_t) + \delta m^{\rm NS}_t\right]\omega_- \\ & - \left[\frac{m_t}{2}(\delta Z^{R,{\rm NS}}_t + \delta Z^{L^+,{\rm NS}}_t) + \delta m^{\rm NS}_t\right]\omega_+\ .\end{aligned}$$

For the THDM the renormalized constants and counterterms expressed in terms of unrenormalized self-energies can be found in Ref. [9].

B. Higgs tadpole

The radiative correction influence the Higgs potential [6] such that its vacuum expectation value V is shifted. Since V is not a physical quantity, its definition at the one-loop level is arbitrary. In order to correct for this shift, one introduces a counterterm δt to the vacuum expectation value of the Higgs field, such that the Higgs field one-point vertex and the one-loop tadpole contribution T defined in Fig. 4 cancel, i.e., $T + \delta t = 0$. This has the advantage, at the tree level, that the tadpoles never enter a calculation that does not involve other observables of the Higgs sector.

The one-loop tadpole contributions of the nonstandard Higgs field from the diagrams of Fig. 4 lead in the 't Hooft–Feynman gauge to the expressions

$$\begin{aligned} T^{\rm NS} &= \frac{e}{64\pi^2 S_W M_W}\left\{ \left(-6M^2_{H_1} + AM^2_{H_0}\tan\beta\right)\frac{A_0(M_{H_1})}{2} - (2M^2_{H_1} + 4M^2_{H_2} \right. \\ &\qquad \left. - AM^2_{H_0}\tan\beta)\frac{A_0(M_{H_2})}{2} - (2M^2_{H_1} + 4M^2_{\Phi} - AM^2_{H_0}\tan\beta)A_0(M_{\Phi})\right\} \\ &= \delta t^{\rm NS} = \frac{-2S_W M_W M^2_{H_0}}{e}\frac{\delta t^{\rm NS}}{t}\ . \end{aligned}$$

In this paper, $A = \tan 2\alpha$. The definition of the one-point functions A_0 can be found in Ref. [8].

C. Vertex correction

In the 't Hooft–Feynman gauge, all the one-loop vertex diagrams of the $t\bar{t}H_0$ in the THDM have already been given in Ref. [9] and will not be repeated here. Note that by using Ref. [9] here one of three external fields is off shell, such as the s-channel Higgs fields, since corrections containing only virtual gauge bosons and fermions in the $H_0H_0H_0$ vertex are identical in the THDM and MSM given in [7]. Therefore we need only calculate virtual weak corrections within the THDM, more precisely only those involving the five Higgs bosons in Fig. 5. The one-loop corrections to the amplitude can be written as

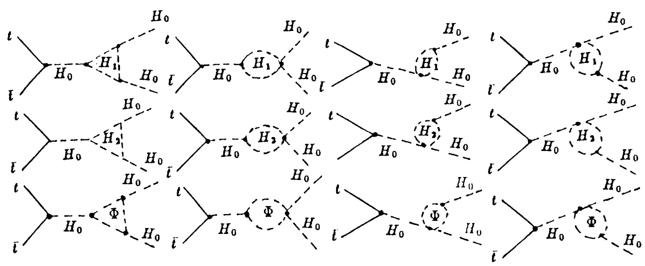

FIG. 5. Nonstandard $H_0H_0H_0$ vertex corrections diagrams.

$$
\begin{aligned}
\delta M^{\rm NS}_{H_0H_0H_0} = \frac{\alpha g_{H_0H_0H_0} g_{ttH_0}}{16\pi S_W^2 M_W^2} \frac{-iM_0}{(s-M_{H_0}^2)} \Bigg\{ & \left[\frac{-3M_{H_1}^4}{2M_{H_0}^2} + \frac{AM_{H_1}^2\tan\beta}{2} - \frac{A^2M_{H_0}^2\tan^2\beta}{24}\right][2B_0(1)+B_0(1')] \\
& + \left[\frac{-1}{6M_{H_0}^2}(M_{H_1}^4 + 4M_{H_1}^2M_{H_2}^2 + 4M_{H_2}^4) + \frac{A\tan\beta}{6}(M_{H_1}^2 + 2M_{H_2}^2)\right. \\
& \left. - \frac{A^2M_{H_0}^2\tan^2\beta}{24}\right][2B_0(2)+B_0(2')] + \left[\frac{-1}{3M_{H_0}^2}(M_{H_1}^4 + 4M_{H_1}^2M_\Phi^2 + 4M_{H_\Phi}^4)\right. \\
& \left. + \frac{A\tan\beta}{3}(M_{H_1}^2 + 2M_\Phi^2) - \frac{A^2M_{H_0}^2\tan^2\beta}{12}\right][2B_0(\Phi)+B_0(\Phi')] \\
& + \left[\frac{9M_{H_1}^6}{2M_{H_0}^2} - \frac{9AM_{H_1}^4\tan\beta}{4} + \frac{3A^2M_{H_0}^2M_{H_1}^2\tan^2\beta}{8} - \frac{A^3M_{H_0}^4\tan^3\beta}{48}\right][C_0(1)+C_0(1')] \\
& + \left[\frac{1}{6M_{H_0}^2}(M_{H_1}^6 + 6M_{H_1}^4M_{H_2}^2 + 12M_{H_1}^2M_{H_2}^4 + 8M_{H_2}^6)\right. \\
& \left. - \frac{A\tan\beta}{4}(M_{H_1}^4 + 4M_{H_1}^2M_{H_2}^2 + 4M_{H_2}^4) + \frac{A^2M_{H_0}^2\tan^2\beta}{8}(M_{H_1}^2 + 2M_{H_2}^2) - \frac{A^3M_{H_0}^4\tan^3\beta}{48}\right][C_0(2)+C_0(2')] \\
& + \left[\frac{1}{3M_{H_0}^2}(M_{H_1}^6 + 6M_{H_1}^4M_\Phi^2 + 12M_{H_1}^2M_\Phi^4 + 8M_\Phi^6) - \frac{A\tan\beta}{2}(M_{H_1}^4 + 4M_{H_1}^2M_\Phi^2 + 4M_\Phi^4)\right. \\
& \left. + \frac{A^2M_{H_0}^2\tan^2\beta}{4}(M_{H_1}^2 + 2M_\Phi^2) - \frac{A^3M_{H_0}^4\tan^3\beta}{24}\right][C_0(\Phi)+C_0(\Phi')] \\
& + \left[\delta Z_e^{\rm NS} - \frac{\delta S_W^{\rm NS}}{S_W} + \frac{\delta M_{H_0}^{2\rm NS}}{M_{H_0}^2} - \frac{\delta M_W^{2\rm NS}}{2M_W^2} + \frac{3}{2}\delta Z_{H_0}^{\rm NS} + \frac{\delta t^{\rm NS}}{t}\right]\Bigg\}.
\end{aligned}
$$

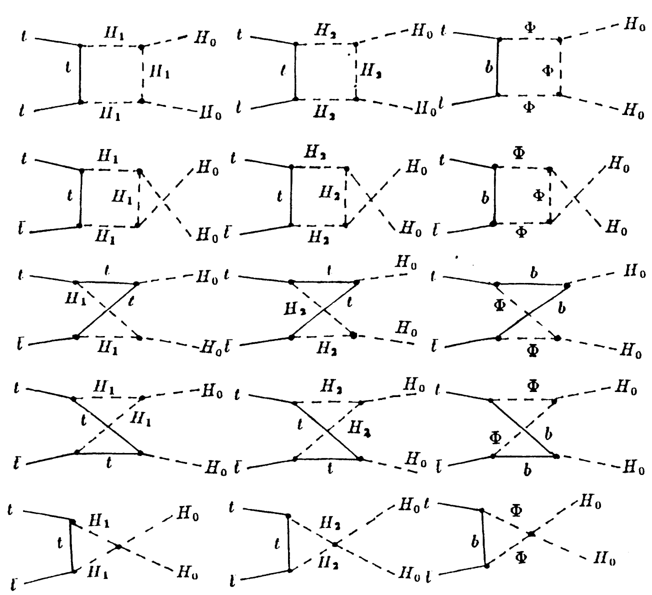

FIG. 6. Nonstandard box graphs.

The self-energies in the THDM were already calculated. Complete explicit expressions for the unrenormalized self-energies and the renormalization constants are listed in Refs. [9,10].

The arguments of the invariant integrals are

$$B_0(1) = B_0(M_{H_0}^2, M_{H_1}, M_{H_1}) \ , \quad B_0(1') = B_0(s, M_{H_1}, M_{H_1}) \ ,$$

$$B_0(2) = B_0(M_{H_0}^2, M_{H_2}, M_{H_2}) \ , \quad B_0(2') = B_0(s, M_{H_2}, M_{H_2}) \ ,$$

$$B_0(\Phi) = B_0(M_{H_0}^2, M_{\Phi}, M_{\Phi}) \ , \quad B_0(\Phi') = B_0(s, M_{\Phi}, M_{\Phi}) \ ,$$

$$C_0(1) = C_0(p_3, -p_3 - p_4, M_{H_1}, M_{H_1}, M_{H_1}) \ , \quad C_0(1') = C_0(-p_3, p_3 + p_4, M_{H_1}, M_{H_1}, M_{H_1}) \ ,$$

$$C_0(2) = C_0(p_3, -p_3 - p_4, M_{H_2}, M_{H_2}, M_{H_2}) \ , \quad C_0(2') = C_0(-p_3, p_3 + p_4, M_{H_2}, M_{H_2}, M_{H_2}) \ ,$$

$$C_0(\Phi) = C_0(p_3, -p_3 - p_4, M_{\Phi}, M_{\Phi}, M_{\Phi}) \ , \quad C_0(\Phi') = C_0(-p_3, p_3 + p_4, M_{\Phi}, M_{\Phi}, M_{\Phi}) \ .$$

The definition of the two- and three-point functions B_0 and C_0 can be found in Ref. [8].

D. Box correction

The additional Higgs contributions in the box diagrams as shown in Fig. 6 can be written

$$\delta M_{\text{box}}^{\text{NS}} = \sum_{i=1}^{i=15} \delta M_{Bi}^{\text{NS}} \ .$$

The analytical expressions of $\delta M_{Bi}^{\text{NS}}$ denoted by the internal particles are given in terms of the invariant integrals C and D as

$$\delta M_{B1}^{\text{NS}} = \frac{i\alpha^2 m_t^2}{16 S_W^4 M_W^4} \left\{ \left[\frac{A^2 M_{H_0}^4}{4} - 3A M_{H_0}^2 M_{H_1}^2 \cot\beta + 9 M_{H_1}^4 \cot^2\beta \right] [m_t(D_0^1 - D_{11}^1)M_0 - D_{13}^1 M_4] \right\} ,$$

$$\begin{aligned} \delta M_{B2}^{\text{NS}} = \frac{i\alpha^2 m_t^2}{16 S_W^4 M_W^4} \Bigg\{ \Bigg[& -\frac{A^2 M_{H_0}^4}{4} + A M_{H_0}^2 M_{H_1}^2 \cot\beta + 2A M_{H_0}^2 M_{H_2}^2 \cot\beta - M_{H_1}^4 \cot^2\beta \\ & -4 M_{H_1}^2 M_{H_2}^2 \cot^2\beta - 4 M_{H_2}^4 \cot^2\beta \Bigg] [m_t(D_0^2 + D_{11}^2)M_0 + D_{13}^2 M_4] \Bigg\} , \end{aligned}$$

$$\begin{aligned} \delta M_{B3}^{\text{NS}} = \frac{i\alpha^2}{16 S_W^4 M_W^4} \Bigg\{ & (M_{H_1}^4 + 4 M_{H_1}^2 M_{\Phi}^2 + 4 M_{\Phi}^2)\{2 m_b^2 m_t D_0^3 M_0 - (m_t^2 \cot^2\beta + m_b^2 \tan^2\beta)[D_{13}^3(M_4 - M_5)] \\ & - m_t^3 \cot^2\beta [D_{11}^3(M_0 - M_1) + 2 D_{12}^3 M_1] - m_b^2 m_t \tan^2\beta [D_{11}^3(M_0 + M_1) - 2 D_{12}^3 M_1]\} \\ & + A M_{H_0}^2 m_t^2 \left(2 M_{\Phi}^2 \cot\beta + M_{H_1}^2 \cot\beta - \frac{A M_{H_0}^2}{4} \right) \{D_{13}^3(M_4 - M_5) + m_t[D_{11}^3(M_0 - M_1) - 2 D_{12}^3 M_1]\} \\ & + A M_{H_0}^2 m_b^2 \left(2 M_{\Phi}^2 + M_{H_1}^2 - \frac{A M_{H_0}^2 \tan\beta}{4} \right) \{m_t \tan^3\beta [D_{11}^3(M_0 + M_1) - 2 D_{12}^3 M_1] + \tan^3\beta D_{13}^3(M_4 + M_5) \\ & - 2 m_t \tan\beta D_0^3 M_0\} \Bigg\} , \end{aligned}$$

$$\delta M_{B4}^{\text{NS}} = \delta M_{B1}^{\text{NS}}(p_3 \leftrightarrow p_4) \ ,$$

$$\delta M_{B5}^{\text{NS}} = \delta M_{B2}^{\text{NS}}(p_3 \leftrightarrow p_4) \ ,$$

$$\delta M_{B6}^{\text{NS}} = \delta M_{B3}^{\text{NS}}(p_3 \leftrightarrow p_4) \ ,$$

$$\delta M_{B7}^{\rm NS}=\frac{i\alpha^2 m_t^3\cot\beta}{16S_W^4M_W^4}\left(3M_{H_1}^2\cot\beta-\frac{AM_{H_0}^2}{2}\right)\left\{M_{H_0}^2(D_{11}^{1'}-D_{12}^{1'})M_0-(D_{12}^{1'}-D_{13}^{1'})M_6\right.$$

$$+m_t[(D_0^{1'}+2D_{11}^{1'}-3D_{12}^{1'})M_2-2(D_{12}^{1'}-D_{13}^{1'})M_4]$$

$$\left.+2m_t^2(D_0^{1'}-D_{12}^{1'})M_0-C_0(p_2-p_3-p_4,p_4,m_t,M_{H_1},M_{H_1})M_0\right\}\ ,$$

$$\delta M_{B8}^{\rm NS}=\frac{i\alpha^2 m_t^3\cot\beta}{16S_W^4M_W^4}\left(\frac{AM_{H_0}^2}{2}-M_{H_1}^2\cot\beta-2M_{H_2}^2\cot\beta\right)\left\{M_{H_0}^2(D_{11}^{2'}-D_{12}^{2'})M_0+m_t^2(D_0^{2'}+2D_{12}^{2'})M_0\right.$$

$$\left.-m_t(D_0^{2'}+2D_{11}^{2'}-2D_{12}^{2'})M_2+(D_{12}^{2'}-D_{13}^{2'})(2m_tM_4-M_6)-C_0(p_2-p_3-p_4,p_4,m_t,M_{H_2},M_{H_2})M_0\right\}\ ,$$

$$\delta M_{B9}^{\rm NS}=\frac{i\alpha^2}{16S_W^4M_W^4}\left\{m_b^4\left(M_{H_1}^2+2M_\Phi^2-\frac{AM_{H_0}^2\tan\beta}{2}\right)\{[4D_0^{3'}M_0-2\tan^2\beta(D_{12}^{3'}-D_{13}^{3'})(M_4-M_5)\right.$$

$$-2\tan^2\beta m_tD_{12}^{3'}(M_0-M_1)+\tan^2\beta(D_0^{3'}+2D_{11}^{3'}-2D_{12}^{3'})(M_2+M_3)]\}+2m_b^2(M_{H_1}^2+2M_\Phi^2)$$

$$\times[m_tM_{H_0}^2(D_{11}^{3'}-D_{12}^{3'})M_0-m_t(D_{12}^{3'}-D_{13}^{3'})M_6-m_t^2D_{12}^{3'}M_2]+m_b^2m_t^2\cot\beta\left(M_{H_1}^2\cot\beta+2M_\Phi^2\cot\beta-\frac{AM_{H_0}^2}{2}\right)$$

$$\times\{(D_0^{3'}+2D_{11}^{3'}-2D_{12}^{3'})(M_2-M_3)-2(D_{12}^{3'}-D_{13}^{3'})(M_4-M_5)-2m_t\cot\beta D_{12}^{3'}(M_0+M_1)\}$$

$$\left.-2m_b^2m_t\left(M_{H_1}^2+2M_\Phi^2-\frac{AM_{H_0}^2\tan\beta}{2}\right)C_0(p_2-p_3-p_4,p_4,m_b,M_\Phi,M_\Phi)M_0\right\}\ ,$$

$$\delta M_{B10}^{\rm NS}=\delta M_{B7}^{\rm NS}(p_3\leftrightarrow p_4)\ ,$$

$$\delta M_{B11}^{\rm NS}=\delta M_{B8}^{\rm NS}(p_3\leftrightarrow p_4)\ ,$$

$$\delta M_{B12}^{\rm NS}=\delta M_{B9}^{\rm NS}(p_3\leftrightarrow p_4)\ ,$$

$$\delta M_{B13}^{\rm NS}=\frac{i\alpha^2 m_t^3\cot\beta}{16S_W^4M_W^4}\left(\frac{AM_{H_0}^2}{2}-3M_{H_1}^2\cot\beta\right)[(C_0-C_{11})(-p_1,p_1+p_2,m_t,M_{H_1},M_{H_1})]M_0\ ,$$

$$\delta M_{B14}^{\rm NS}=\frac{i\alpha^2 m_t^3\cot\beta}{16S_W^4M_W^4}\left(\frac{AM_{H_0}^2}{2}+M_{H_1}^2\cot\beta+2M_{H_2}^2\cot\beta\right)[(C_0-C_{11})(-p_1,p_1+p_2,m_t,M_{H_2},M_{H_2})]M_0\ ,$$

$$\delta M_{B15}^{\rm NS}=\frac{i\alpha^2}{16S_W^4M_W^4}\left\{m_t^3\cot\beta\left(\frac{AM_{H_0}^2}{2}-M_{H_1}^2\cot\beta-2M_\Phi^2\cot\beta\right)[2C_{12}M_1-C_{11}(M_0+M_1)-2m_b^2m_tC_0M_0]\right.$$

$$\times(-p_1,p_1+p_2,m_b,M_\Phi,M_\Phi)+m_b^2m_t\tan\beta\left(\frac{AM_{H_0}^2}{2}\tan\beta-M_{H_1}^2-2M_\Phi^2\right)$$

$$\left.\times[C_{11}(M_1-M_0)-2C_{12}M_1](-p_1,p_1+p_2,m_b,M_\Phi,M_\Phi)\right\}\ ,$$

with

$$D_{i,j}^1=D_{i,j}(-p_1,p_1+p_2,-p_4,m_t,M_{H_1},M_{H_1},M_{H_1})\ ,$$

$$D_{i,j}^{1'}=D_{i,j}(p_3,p_2-p_3-p_4,p_4,m_t,m_t,M_{H_1},M_{H_1})\ ,$$

$$D^2_{i,j} = D_{i,j}(-p_1, p_1+p_2, -p_4, m_t, M_{H_2}, M_{H_2}, M_{H_2}) \,,$$

$$D^{2'}_{i,j} = D_{i,j}(p_3, p_2-p_3-p_4, p_4, m_t, m_t, M_{H_2}, M_{H_2}) \,,$$

$$D^3_{i,j} = D_{i,j}(-p_1, p_1+p_2, -p_4, m_b, M_\Phi, M_\Phi, M_\Phi) \,,$$

$$D^{3'}_{i,j} = D_{i,j}(p_3, p_2-p_3-p_4, p_4, m_b, m_b, M_\Phi, M_\Phi) \,.$$

IV. RESULTS AND DISCUSSION

For the numerical evaluations we use the set of parameters which is from more recent published values [4]:

$$\alpha_{\rm em} = 1/137.035\,989\,5 \,, \quad G_F = 1.166\,37\times10^{-5}\ {\rm GeV}^{-2} \,, \quad M_Z = 91.188\ {\rm GeV} \,,$$

$$m_e = 0.510\,999\,06\ {\rm MeV} \,, \quad m_\mu = 0.105\,658\,39\ {\rm GeV} \,, \quad m_\tau = 1.7841\ {\rm GeV} \,,$$

$$m_u = 41\ {\rm MeV} \,, \quad m_d = 41\ {\rm MeV} \,, \quad m_s = 150\ {\rm MeV} \,,$$

$$m_c = 1.5\ {\rm GeV} \,, \quad m_b = 4.7\ {\rm GeV} \,.$$

We use the known Fermi constant G_F as numerical input, accurately measured in muon decay. The mass of the W boson is calculated from the relation

$$M_W^2\left(1-\frac{M_W^2}{M_Z^2}\right) = \frac{\pi\alpha_{\rm em}}{\sqrt{2}G_F}\frac{1}{1-\Delta r_{\rm THDM}} \,.$$

Here $\Delta r_{\rm THDM}$ depends on the weak corrections to this decay calculated in the THDM, particularly on the top quark and unknown Higgs boson masses [10].

For the numerical analysis, for the Higgs sector of the THDM we choose β, α, M_{H_0}, M_{H_1}, M_{H_2}, $M_{\Phi^\pm}$, and m_t as input parameters and set $\alpha=\beta$. The experimental data from CP violation and K and B physics [11] as well as perturbative and unitarity considerations [12] can indicate

$$0.5 \le \tan\beta \le 100 \,, \quad 0 < M_{H_1}, M_{H_2} \le 1\ {\rm TeV} \,,$$

$$M_\Phi \ge \tfrac{1}{2}M_Z \,.$$

Therefore we restrict ourselves to values well within the allowed parameter region. We have chosen $\tan\beta = 70$.

Since in this paper we are only interested in deviations of the THDM from the MSM, we split all corrections in

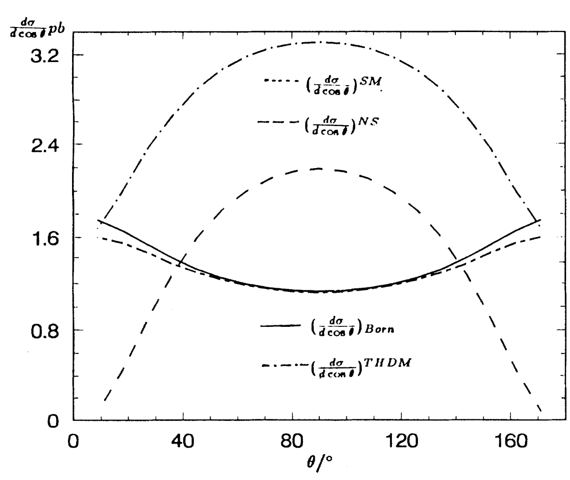

FIG. 7. Angular dependence of the differential cross section for the one-loop corrections of the MSM, the one-loop corrections of the THDM, and the additional Higgs boson one-loop corrections with $m_t = 175$ GeV, $M_{H_1} = 50$ GeV, $M_{H_2} = M_\Phi = 150$ GeV, $M_{H_0} = 400$ GeV, and $\sqrt{s} = 1$ TeV.

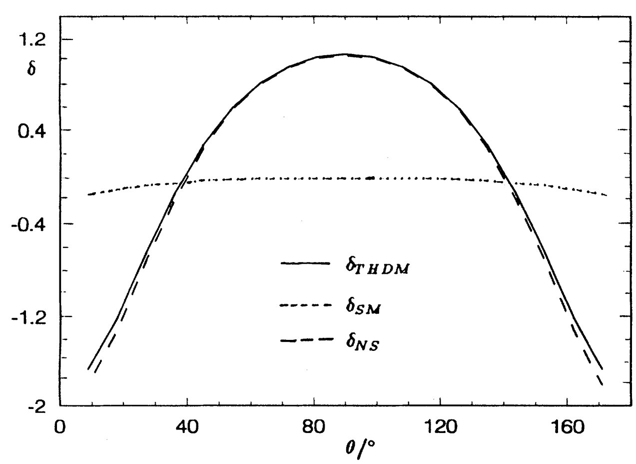

FIG. 8. Angular dependence of δ. Same signature as in Fig. 7.

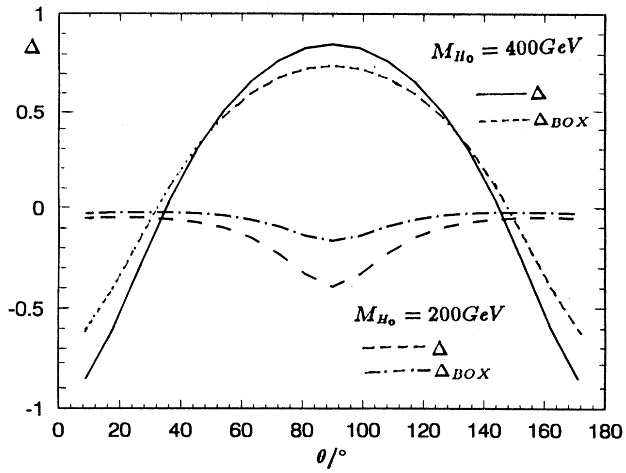

FIG. 9. Angular dependence of Δ for $M_{H_0} = 200$ GeV (dashed line) and $M_{H_0} = 400$ GeV (solid line) with $m_t = 175$ GeV, $M_{H_1} = 50$ GeV, and $M_{H_2} = M_\Phi = 300$ GeV at $\sqrt{s} = 1$ TeV. The long-dashed line is the nonstandard box correction Δ for $M_{H_0} = 200$ GeV. The short-dashed line is the nonstandard box correction Δ for $M_{H_0} = 400$ GeV.

a standard model (MSM) part and a nonstandard (NS) part. The latter is defied as the difference of the relevant quantities in the THDM and MSM. We introduce the quantities

$$\Delta = \frac{\left(\frac{d\sigma}{d\cos\theta}\right)^{\mathrm{THDM}} - \left(\frac{d\sigma}{d\cos\theta}\right)^{\mathrm{MSM}}}{\left(\frac{d\sigma}{d\cos\theta}\right)_{\mathrm{Born}}},$$

which directly give the nonstandard corrections.

In Fig. 7 we give the differential cross section in lowest order, $(\frac{d\sigma}{d\cos\theta})_{\mathrm{Born}}$, the one including the complete one-loop corrections $(\frac{d\sigma}{d\cos\theta})^{\mathrm{SM}}$ in the soft photon approximation with soft photon cutoff $\Delta E = 0.1E$ in the MSM, the one including the one-loop corrections $(\frac{d\sigma}{d\cos\theta})^{\mathrm{THDM}}$ in the THDM, and the one including the one-loop correction of the additional Higgs bosons, $(\frac{d\sigma}{d\cos\theta})^{\mathrm{NS}}$, to the process $t\bar{t}\to H_0H_0$ with $m_t = 175$ GeV, $M_{H_1} = 50$ GeV, $M_{H_2} = M_\Phi = 150$ GeV, and $M_{H_0} = 400$ GeV (at $\sqrt{s} = 1$ TeV) and show the contributions of different δ in Fig. 8. The origin of the large angular-dependent corrections is due to the nonstandard corrections δ_{NS}. The δ_{SM} corrections exhibit a very weak angular dependence, which gets only larger corrections in the forward and backward directions; the nonstandard corrections, however, vary strongly in our considering case.

The angular dependence of Δ for different M_{H_0} with M_{H_2} was set equal to M_Φ and is plotted in Fig. 9. The dashed line is for $M_{H_0} = 200$ GeV and solid line

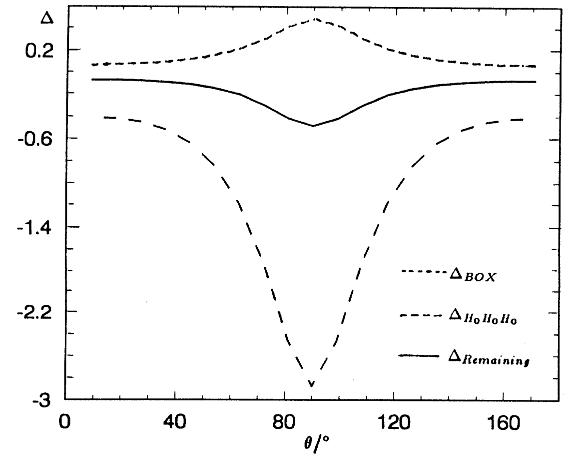

FIG. 11. Different contributions to Δ as described in Fig. 10.

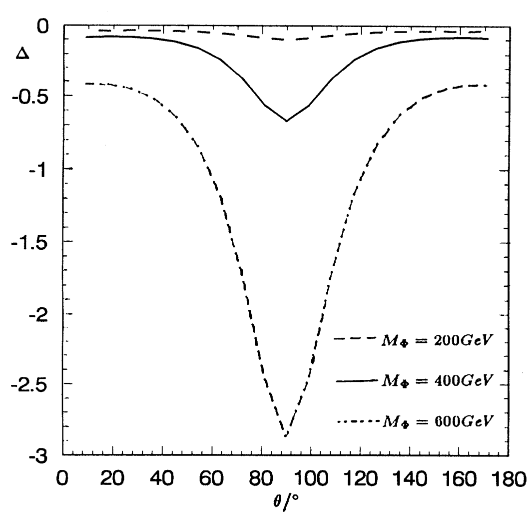

FIG. 10. Angular dependence of Δ for various masses of Φ with $m_t = 175$ GeV, $M_{H_1} = 50$ GeV, and $M_{H_0} = 200$ GeV at $\sqrt{s} = 1$ TeV.

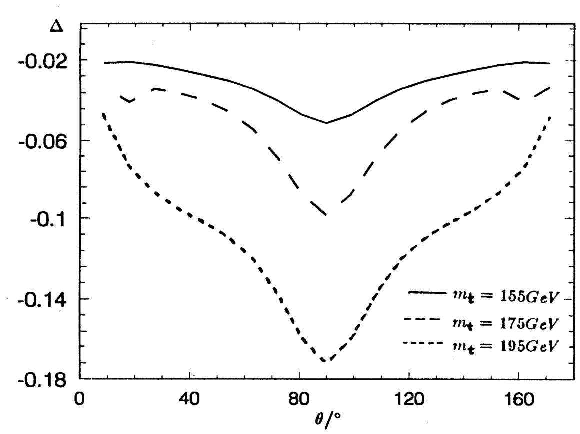

FIG. 12. Angular dependence of Δ for various masses of the top quark with $M_{H_0} = 200$ GeV, $M_{H_1} = 50$ GeV, and $M_{H_2} = M_\Phi = 200$ GeV at $\sqrt{s} = 1$ TeV.

for $M_{H_0} = 400$ GeV. The corrections go upturned for $M_{H_0} = 200$ GeV, whereas in turn the corrections for $M_{H_0} = 400$ GeV are upside down. The reason for this difference is mainly negative box corrections (see Fig. 9) for $M_{H_0} = 200$ GeV, but the corrections for $M_{H_0} = 400$ GeV become negative in the forward and backward directions and become positive between 36° and 140°. The Higgs boson mass dependence of the corrections strengthens for $M_{H_0} = 400$ GeV. The nonstandard corrections become rather big and the largest effect is from the nonstandard box corrections as shown in Fig. 9. This is due to the fact that the lowest-order differential cross section, for larger M_{H_0} (as $M_{H_0} = 400$ GeV), is of order $1/s$ for all scattering angles. An analysis of the box contributions shows that these involve terms behaving as $1/t$ or $1/u$ for $M^2_\Phi(M^2_{H_2}) \ll |t| \ll s$ and approaching a constant of the order of $\frac{\alpha}{\pi M^2_{H_2}}$ or $\frac{\alpha}{\pi M^2_\Phi}$ for $|t| \ll M^2_\Phi(M^2_{H_2})$. This behavior of the box corrections is familiar from many other (t- and u-channel) processes. Thus the box corrections are large because of the independent scattering angles of the lowest-order differential cross section.

In Fig. 10 we show Δ as a function of angle when $M_{H_1} = 50$ GeV, $m_t = 175$ GeV, $M_{H_0} = 200$ GeV, and $M_{H_2} = M_\Phi = 200$, 400, and 600 GeV, respectively. The nonstandard corrections become particularly large if M_Φ is large and negative. The large corrections display an angular dependence. In order to unravel the origin of the large corrections, we show the separate contributions to the Δ in Fig. 11. We give the box corrections, the $H_0H_0H_0$ vertex corrections, and the sum of the remaining corrections (self-energies, $t\bar{t}H_0$ vertex of the s, t, and u channels). We find in the calculation that the largest effect of the nonstandard corrections is from cubic Higgs vertex corrections. The reason is that the large nonstandard Higgs boson masses enhance the corrections by the couplings of H_0 with H_2 and Φ [7]. If the nonstandard Higgs boson masses are not very heavy, the remaining and box corrections partially cancel, resulting in a total correction from the cubic Higgs vertex corrections.

In Fig. 12 we give the nonstandard corrections Δ for $M_{H_0} = 200$ GeV; the values of m_t have been chosen such that the allowed range is covered. Varying the top mass within 155 GeV $\leq m_t \leq$ 195 GeV, the short-dashed line (with $m_t = 195$ GeV) has the large corrections of the angular dependence. This is due to contributions $\propto m_t/M_W$ which are enhanced.

We emphasize that Δ is negative for most of the allowed parameter case. So the MSM corrections are in general partially canceled or even made into negative ones.

V. CONCLUSION

We have calculated the one-loop corrections to the process $t\bar{t} \to H_0H_0$ arising from a two Higgs doublet. A numerical evaluation of these nonstandard corrections has been given for the case of Higgs boson pair production. The calculation shows that the nonstandard corrections are generally negative for a large top mass and grow with the additional Higgs boson mass M_Φ. The dominating difference between the THDM and MSM arises not only from the nonstandard self-energies and renormalization constants, which will always strengthen for the coupling of H_0 with heavy H_2 and Φ, but also from the nonstandard box and cubic Higgs vertex corrections. At the large M_{H_0}, m_t, and M_Φ, the angular dependence of radiative corrections yields very large contributions in our THDM.

ACKNOWLEDGMENTS

The work was supported in part by the National Natural Science Foundation of China.

[1] Particle Data Group, K. Hikasa *et al.,* Phys. Rev. D **45**, S1 (1992); L. Rolandi, in *Proceedings of the 26th International Conference on High Energy Physics*, Dallas, Texas, 1992, edited by J. Sanford, AIP Conf. Proc. No. 272 (AIP, New York, 1993).

[2] CDF Collaboration, F. Abe *et al.,* Phys. Rev. D **50**, 2966 (1992).

[3] S. L. Glashow and S. Weinberg, Phys. Rev. D **15**, 1958 (1977); G. Mrachio, R. Gutto, G. Sartori, and F. Strocchi, Nucl. Phys. **B163**, 221 (1980).

[4] Particle Data Group, L. Montanet *et al.,* Phys. Rev. D **50**, 1173 (1994).

[5] Kalpana, J. Kallianpur, Phys. Lett. B **215**, 392 (1988).

[6] A. Denner, Fortschr. Phys. **41**, 4 (1993); **41**, 307 (1993); K. I. Aoki, Z. Hioki, R. Kawabe, M. Konuma, and T. Muta, Prog. Theor. Phys. **64**, 707 (1980); **65**, 1001 (1981).

[7] M. L. Qian, M. Sci. thesis, U.S.T.C., 1995.

[8] G. 't Hooft and M. Veltman, Nucl. Phys. **B153**, 365 (1979); G. Passarino and M. Veltman, *ibid.* **B160**, 151 (1979).

[9] X. X. Chen, W. G. Ma, Y. Y. Liu, L. Z. Sun, and C. H. Chang, Phys. Rev. D **50**, 4563 (1994); W. G. Ma and L. Z. Sun, *ibid.* **51**, 2279 (1995).

[10] W. Hollik, Z. Phys. C **32**, 291 (1986); **37**, 569 (1988).

[11] L3 Collaboration, O. Adriani *et al.,* Phys. Rep. **236**, 1 (1993); W. Hollik, Z. Phys. C **37**, 569 (1988); J. F. Gunion and B. Grzadkowski, Phys. Lett. B **243**, 301 (1990); D. Cocolicchio and J.-R. Cudell, *ibid.* **245**, 591 (1990); V. Barger, J. L. Hewett, and R. J. N. Phillips, Phys. Rev. D **41**, 3421 (1990).

[12] H. Huffel and G. Pocsik, Z. Phys. C **8**, 13 (1981); J. Maalampi, J. Sirkka, and I. Vilja, Phys. Lett. B **265**, 371 (1991).